Alpha-particle scattering from ^{6}Li near the α-d breakup threshold

C. Samanta, Sudip Ghosh, and M. Lahiri
Saha Institute of Nuclear Physics, 1/AF, Bidhan Nagar, Calcutta 700 064, India

S. Ray
Department of Physics, Kalyani University, Kalyani 741 235, India

S. R. Banerjee
Variable Energy Cyclotron Center, 1/AF Bidhan Nagar, Calcutta 700 064, India
(Received 23 July 1990; revised manuscript received 23 August 1991)

The ^{6}Li(α,α') reaction was studied at $E_\alpha = 50$ MeV. The angular distribution of the continuum region near the ^{6}Li$\rightarrow\alpha+d$ breakup threshold (1.475 MeV) was measured for $\theta_{lab} = 7°-40°$. The data were analyzed in terms of plane-wave and distorted-wave impulse approximation calculations. To study the possible effects of recombination of the breakup clusters in the exit channel, distorted-wave Born approximation calculations were also performed.

PACS number(s): 25.55.Ci

I. INTRODUCTION

The origin of the continuum near the breakup threshold in the scattering of an energetic projectile from ^{6}Li is an interesting problem. The ^{6}Li nucleus is of special interest because it has a predominant cluster structure with a very low breakup threshold. The cluster structure of ^{6}Li has been the subject of a large number of theoretical and experimental investigations. Target breakup reactions induced by various projectiles like protons, deuterons, alphas, electrons, and pions have confirmed the α-d and ^{3}He-t cluster structure of ^{6}Li [1–6]. In particular, the low breakup threshold (1.475 MeV) of ^{6}Li$\rightarrow\alpha+d$ has provided the opportunity to study the breakup reaction mechanism and the structure of ^{6}Li both at high as well as low incident energies. In the last few years, with the advent of high-energy ^{6}Li-projectile beams, the α-d cluster structure of ^{6}Li has been studied with renewed vigor through inclusive [7] and exclusive measurements [8] of projectile breakup reactions. All these studies have reasonably established that the ^{6}Li$\rightarrow\alpha+d$ relative wave function is of $2s$ character, and the α-d probability in the ground state of ^{6}Li is ~ 0.73 [5]. Recently, for the ^{6}Li(p,p') reaction at 65 and 80 MeV, the angular distribution of the breakup cross section was measured near the α-d breakup threshold [9]. Although quasifree (QF) scattering is found to play an active role here, a significant deviation from the theory was observed at the forward angles ($\theta_{c.m.} \leq 30°$). The experimental continuum cross sections show a maximum at $\theta_{c.m.} \sim 23.5°$, i.e., at $\theta_{lab} \sim 20°$, below which a dip in the cross section was observed. The data were analyzed in the framework of $p+\alpha$ two-body QF scattering using the plane-wave impulse approximation (PWIA) for the ^{6}Li$(p,p\alpha)^2$H reaction. This analysis failed to account for the observed sharp drop in the cross section at forward angles. It was suggested that at the forward angles the QF scattering is strongly influenced by the final-state interaction (FSI), with the knocked-out α and the spectator d, under the condition of small relative energy, recombining into ^{6}Li, an effect not taken into account in the PWIA.

We have studied the breakup of ^{6}Li near the $\alpha-d$ breakup threshold with the ^{6}Li(α,α') reaction at $E_\alpha = 50$ MeV. Since the ^{6}Li$\rightarrow\alpha+d$ binding energy is very small, the α-d bound-state wave function has a long tail [4]. It has already been observed [10,11] that alpha-induced knockout reactions study the low density tail of the nuclear matter distribution. Protons, on the other hand, are more sensitive to the interior of the target nucleus. Therefore, a comparison of (p,p') and (α,α') data is of considerable interest in understanding the reaction mechanism contributing near the α-d breakup threshold. The α particles of 50 MeV are appropriate projectiles for this type of experiment since the α-α two-body scattering cross section in this energy region varies rapidly with both scattering angle and incident energy. If the ^{6}Li(α,α') spectra near the breakup threshold originate from the QF scattering between the projectile α and the bound α cluster, the fluctuating structure of the two-body scattering cross section will be reflected in the data. QF scattering between the projectile α and the bound d is also a possible reaction channel, but its contribution in our data, as explained in Sec. III, is much less than the α-α QF cross section.

At $E_\alpha = 50$ MeV, a predominant cross section for the QF breakup of ^{6}Li$\rightarrow\alpha+d$ has already been confirmed from ^{6}Li$(\alpha,2\alpha)^2$H and ^{6}Li$(\alpha,ad)^4$He in-plane exclusive measurements [1,2]. These experiments, because of the specific choice of the geometry, observed the broken-up α-d pair at large relative energy. By choosing a fixed continuum region near the breakup threshold it is possible to investigate the reaction at small relative α-d energy, and no such data exist for the ^{6}Li(α,α') reaction. Interestingly, in our ^{6}Li(α,α') data we find that at forward angles ($\theta_{lab} < 11°$) the cross section of the fixed continuum

region near the α-d breakup threshold does not show the rise predicted by the impulse-approximation calculations which incorporate a quasifree reaction mechanism. This discrepancy indicates possibly a different reaction mechanism contributing in this region.

In the following sections of this paper we discuss the experimental details and the data (Sec. II), the analyses of the data (Sec. III), and finally the possible implications of our results (Sec. IV).

II. EXPERIMENT

The experiment was carried out at 50 MeV incident alpha energy using the unanalyzed beam available from the Variable Energy Cyclotron at VECC, Calcutta. The beam resolution was about 180 keV. A self-supporting ^{6}Li target was prepared by rolling enriched ^{6}Li ($\sim$99%) metal. The target thickness was 3.20 ± 0.16 mg/cm^2. For particle identification we used several ΔE-E systems with 80–100 μm silicon surface-barrier ΔE detectors and 1.5–2 mm Si(Li) E detectors. However, from the gated spectra it was found that there was no interference from particles emitted through other reaction channels in the energy region we were interested in, i.e., 1 MeV from the ^{6}Li$\rightarrow\alpha+d$ (1.475 MeV) breakup threshold. This is because the various competing processes like $\alpha+^6\text{Li}\rightarrow\alpha+p+n+\alpha$, $\alpha+^6\text{Li}\rightarrow\alpha+p+^5\text{He}$, $\alpha+^6\text{Li}\rightarrow\alpha+^3\text{He}+t$ open at 3.7, 4.59, and 15.8 MeV, respectively. The energy loss of protons or deuterons of energies $\sim$50 MeV in 2 mm of Si detector is too small to cause any interference in the region of interest. The data were taken at 28 angles from 7° to 70° in the laboratory frame. Standard electronics were used and the data were recorded on magnetic tape using a Canberra S-88 multichannel analyzer. The beam current, measured with a Faraday cup, a current integrator, and scalar, was kept between 1 and 40 nA depending on the angle of observation. The data were analyzed using a ND-500 (NORSK-DATA) computer.

A typical spectrum is shown in Fig. 1. Since the alpha particle is an isoscalar probe, the states with isospin $T=0$ are seen to be strongly excited [12]. The arrow between the ^{6}Li(1^+, 0.0 MeV) and ^{6}Li(3^+, 2.185 MeV) states indicates the breakup threshold of ^{6}Li$\rightarrow\alpha+d$ (1.475 MeV). In evaluating the elastic and inelastic cross sections for alpha particles on ^{6}Li, the contributions from the elastic and inelastic peaks of impurities such as ^{16}O, ^{12}C, ^{7}Li, and ^{1}H were subtracted whenever necessary by Gaussian peak fitting. The data for those angles at which the peaks of ^{6}Li were not resolvable from the peaks of impurities were discarded.

The elastic peak of ^{6}Li was fitted by a Gaussian peak-fitting routine. The angular distribution of the ^{6}Li(α,α_0) elastic cross section is plotted in Fig. 2, the errors are the size of the data points, or smaller.

The integrated counts with a fixed energy bin of 1 MeV starting from the α-d breakup threshold (1.475 MeV) were considered for calculating the double differential cross section $d^2\sigma/dE\,d\Omega$. This 1 MeV region of interest is sitting on top of the high energy tail of the 2^+, $T=0$, 4.31 MeV state peak of ^{6}Li. The first excited state peak of ^{6}Li (3^+, $T=0$, 2.185 MeV) also contributes in this region of interest. The contributions from both the 4.31 MeV state and the 2.185 MeV state of ^{6}Li were subtracted separately to obtain the α-d breakup cross section. Both the peaks were not fitted simultaneously because of the presence of the breakup continuum. The breakup continuum is not of a known standard shape. An arbitrary choice of a common background would imply a prior knowledge of the shape of the breakup continuum over

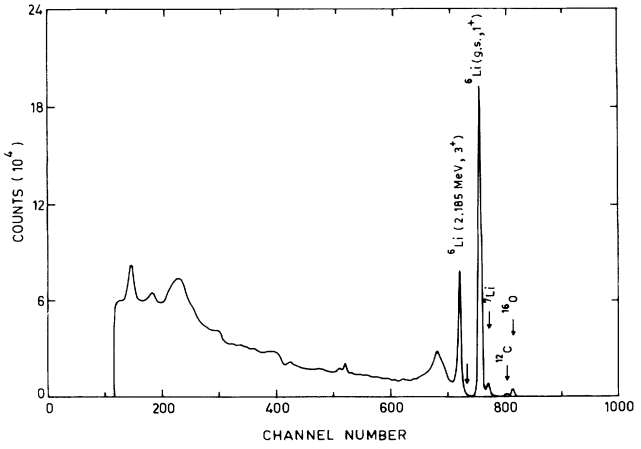

FIG. 1. Spectrum from the ^{6}Li(α,α') reaction at $E_\alpha=50$ MeV for $\theta_{lab}=23.5°$.

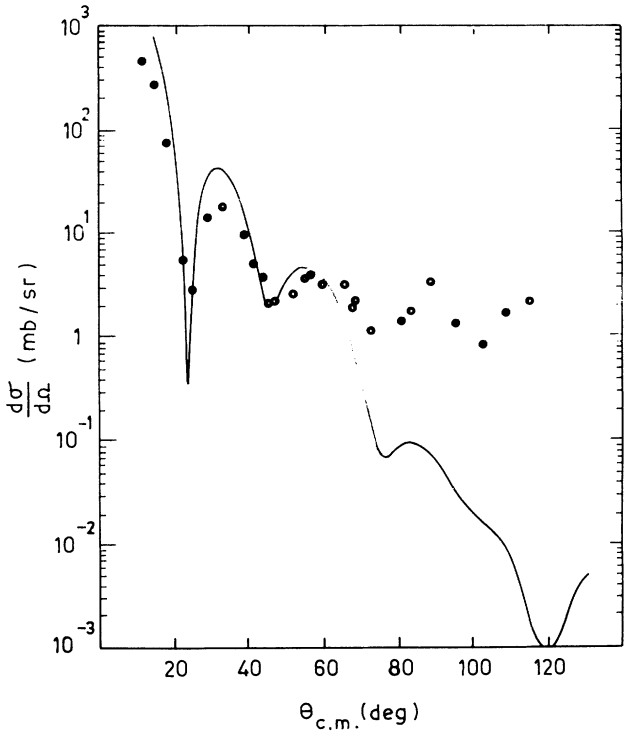

FIG. 2. Elastic angular distribution for α scattering from ^{6}Li at $E_\alpha=50$ MeV. The solid line is an optical model calculation with parameters from Table I.

a large energy range covering both the 4.31 MeV and the first excited state peaks. Also, at larger excitations contributions from high-lying resonance states and other breakup channels may add to the background. It is for this reason that we have restricted our observation of the breakup cross section to the narrow 1 MeV window starting from the breakup threshold. In this 1 MeV region of breakup continuum, contributions from any other reaction channel except the 2.18 and 4.31 MeV excited states of ^{6}Li are practically nonexistent.

The 4.31 MeV state is an unbound state with a large width of 1.7±0.2 MeV [13]. Accordingly, a Breit-Wigner (BW) fit was made to this peak and the contributions from its high-energy tail to our region of interest were subtracted from the total counts. In the fitting procedure we confined our search for the width of the unbound state within the experimental values of 1.7±0.2 MeV. The fit obtained is shown in Fig. 3. Varying the width over the experimentally reported uncertainty of ±0.2 MeV leads to an error of about 2% in our region of interest.

The first excited state of ^{6}Li is also an unbound state but with a small intrinsic width of 0.024±0.002 MeV. This peak was fitted with a Gaussian shape and its contribution was also subtracted from the counts of our region of interest. The subtraction was done both graphically and by means of a Gaussian peak-fitting routine resulting in inelastic yields which in general agreed within 1%. An error matrix analysis of the first excited state peak-fitting procedure gives an error which in general increases with increasing angle. The error is ~0.5% for lower angles and ~1.5% for larger angles, only at one angle (θ_{lab}=40°) the error is ~5%. Figure 3 shows a section of the inclusive α spectrum at 23.5° with the separate contributions from the 2.185 MeV peak (Gaussian fit), the 4.31 MeV peak (BW fit), and the continuum yield obtained after subtraction of the contribution from the above two peaks. The DWIA calculations (see Sec. III) for the α-d breakup cross sections, arbitrarily normalized (spectroscopic factor=0.76) at 23.5°, are also shown. We find that in our 1 MeV region of interest, the DWIA calculations agree with the extracted α-d breakup continuum.

The breakup data were extracted for θ_{lab}=7° to 40° beyond which we could not isolate the 2^+, 4.31 MeV state peak from the impurity peaks. In Fig. 4 we show the angular variations of the counts for the first excited state, the tail of the BW peak in our region of interest (divided by a factor of 10), and the breakup continuum cross section for the same 1 MeV region all plotted in the laboratory frame. The angular distribution of the first excited state peak (3^+, 2.185 MeV) in the center-of-mass frame is shown in Fig. 5.

Figures 6 and 7 represent the double differential cross sections for the continuum yield corresponding to the ex-

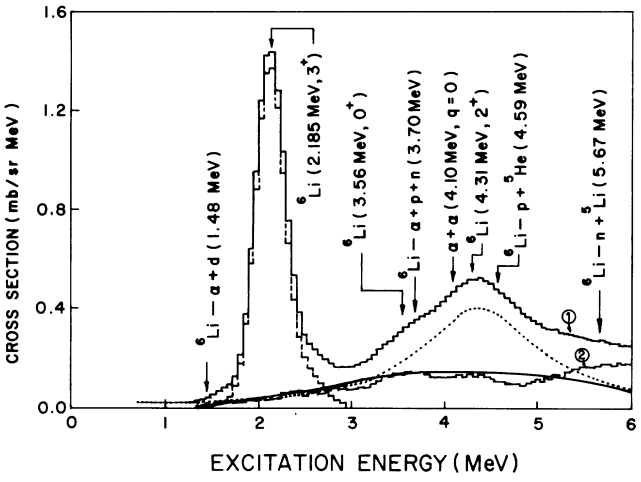

FIG. 3. Spectrum from the ^{6}Li(α,α') reaction at E_α=50 MeV for θ_{lab}=23.5° showing the continuum yield after subtraction of the 2.185 and 4.31 MeV peaks. The experimental data are represented by the upper histogram (1). The dashed line histogram is the Gaussian fit of the 2.185 MeV peak. The dotted line is the BW fit of 4.31 MeV peak obtained with a width of 1.5 MeV. The lower histogram (2) is the continuum yield. The DWIA calculation for ^{6}Li($\alpha,2\alpha$) reaction with normalization constant 0.76 is shown by the full line. The arrows show the positions of the various peaks, the threshold of different reaction channels, and the position of the α-α QF scattering (q=0). The position of the α-d QF scattering is at a higher excitation energy (13.6 MeV).

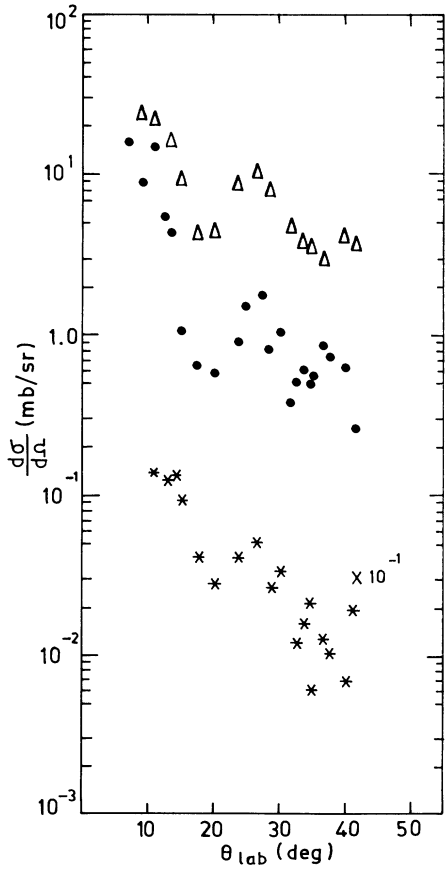

FIG. 4. Angular distribution in the laboratory frame. Δ ^{6}Li(α,α_1) ^{6}Li*, (3^+, 2.185 MeV), ● breakup continuum in the 1.47–2.47 MeV region, * Breit-Wigner tail of 2^+, 4.31 MeV state within 1.47–2.47 MeV region.

citation energy range 1.47–2.47 MeV in the ^{6}Li(α,α') reaction at $E_\alpha=50$ MeV plotted against the laboratory angle (θ_{lab}) and the center-of-mass angle ($\theta_{c.m.}$), respectively. The error bars in Figs. 6 and 7 originate from statistical and systematic errors. These include (i) the error due to the peak subtraction discussed earlier, (ii) the uncertainty in the determination of the solid angle ($\sim$2.5%), and (iii) the uncertainty in the target thickness measurement, the main contribution coming from the estimation of the correction in thickness from contaminants. The error due to this factor was estimated to be about 5%. The total error due to all these factors vary from 9% to 15% for the different experimental points. The data at $\theta_{lab}=7°$ and 9° have relatively larger errors ($\sim$20%) due to the presence of $\alpha+^1$H elastic peak near our region of interest. Also, we could not subtract the BW tail at the angles 7° and 9° because of the presence of the impurity peaks near the 2^+, 4.31 MeV state. Therefore, the continuum cross sections at these two angles should be taken as the upper bound of their values. At larger angles this hydrogen peak no longer interferes with our data. It should be noted that the contribution from sequential decay, which can be seen in exclusive measurements, is completely absent in our data; in our inclusive spectra they appear in the low-energy region, far from our region of interest.

From Figs. 6 and 7 we find that the nature of ^{6}Li(α,α')

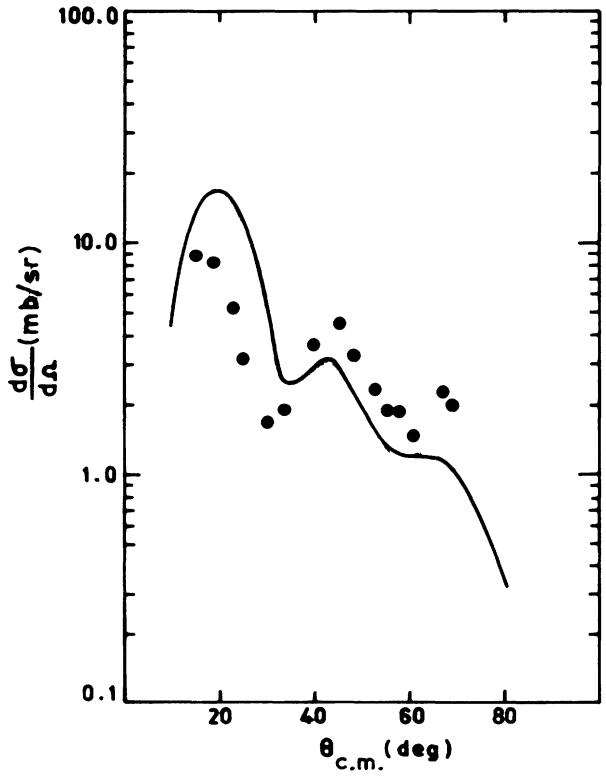

FIG. 5. Angular distribution for the 3^+ (2.185 MeV) excited state of ^{6}Li from the ^{6}Li(α,α_1) reaction at $E_\alpha=50$ MeV. The solid line is the DWBA calculation with deformation parameter $\beta=0.45$ and optical-potential parameters from Table I.

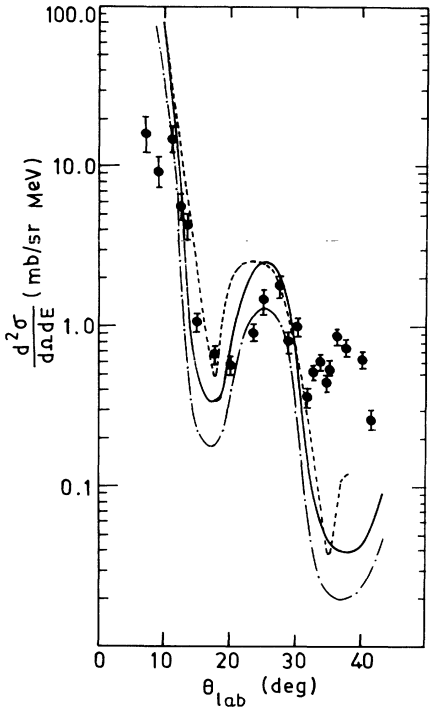

FIG. 6. Double differential cross sections for the continuum yield corresponding to excitation energy of 1.47–2.47 MeV (near the α-d breakup threshold) in the ^{6}Li(α,α') reaction at $E_\alpha=50$ MeV. The curves are the results of PWIA calculation with normalization constant 0.14 ($\cdots$), DWIA calculations with spectroscopic factor 1.8 (——) and spectroscopic factor 1.0 (— · —).

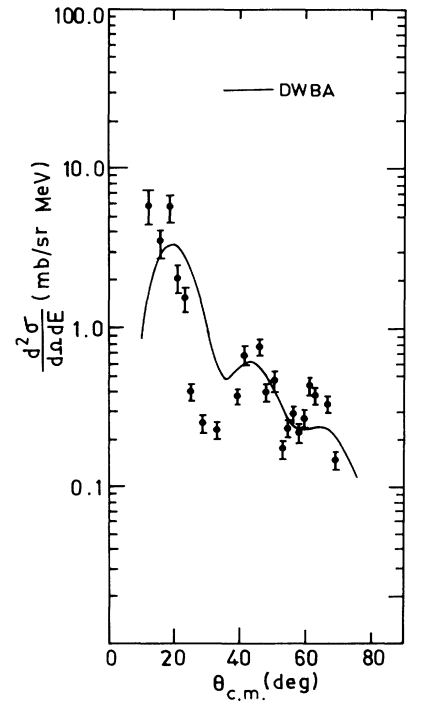

FIG. 7. The same data as in Fig. 6 plotted against center-of-mass angles. DWBA calculations are shown with $\beta=0.19$.

data is quite different from that observed in ^{6}Li(p,p') studies [9]. The (α,α') data show a diffraction structure with the first minimum falling around $\theta_{\text{c.m.}} \sim 30°$. This feature is completely absent in the (p,p') data. At our incident energy alpha-alpha scattering is highly diffractive with considerable structure in its angular distribution whereas proton-alpha scattering is not. As mentioned earlier, this fluctuating structure of the continuum cross section in the ^{6}Li(α,α') data may originate from the quasifree scattering between the projectile and the bound alpha clusters. Therefore in the following section we analyze our data first in the framework of a QF reaction mechanism.

III. ANALYSIS

To investigate the origin of our continuum data near the α-d breakup threshold we have carried out the following analysis.

A. Quasifree scattering

First we consider a quasifree (QF) reaction mechanism. In the QF mechanism the incident projectile interacts with either a bound alpha or a bound deuteron cluster inside the ^{6}Li-target nucleus and this two-body interaction knocks that particular cluster out of the target nucleus while the residual nucleus recoils with the same momentum it had before the interaction. This means that the (α,α') cross section near the breakup threshold originates from either the ^{6}Li$(\alpha,2\alpha)^2$H or ^{6}Li$(\alpha,\alpha d)\alpha$ reaction. Inside the nucleus, the bound cluster has a distribution of relative momentum (q) including zero. At the $q=0$ point, the interaction between the projectile and the bound cluster is almost like a free two-body interaction except for the presence of the binding energy.

For such a QF two-body kinematic calculation, we find that the $q=0$ point for both the α-α and α-d scattering lies very close to the breakup threshold (our region of interest) at the forward angles, and as the observed scattered angle increases, this $q=0$ point moves toward lower scattered alpha energies compared to the $\alpha+^6$Li elastic peak. This can be easily understood because both in $\alpha+\alpha$ or $\alpha+d$ QF scattering the bound α or d target is lighter than the target ^{6}Li. Our window of measurement of continuum cross section is fixed (only 1 MeV from the breakup threshold) and this implies that as the scattering angle increases we are scanning progressively larger values of q for the α-d bound-state wave function (Fig. 8).

In ^{6}Li, the relative orbital angular momentum of the α particle and the deuteron is restricted to $L=0$ or 2 and many previous studies have shown that $L=0$ dominates [5]. The relative momentum wave function, $\Phi(q)$, thus has a maximum at $q=0$ (Fig. 8). Therefore, according to the QF model, in this fixed energy bin one expects relatively larger cross sections at forward angles compared to backward angles. However, in the ^{6}Li(p,p') experiment [9] this expectation was contradicted and a sudden fall of cross section was observed at the forward angles. At first, to understand the trend of our (α,α') data, we did the PWIA analysis as was done in the ^{6}Li(p,p') work.

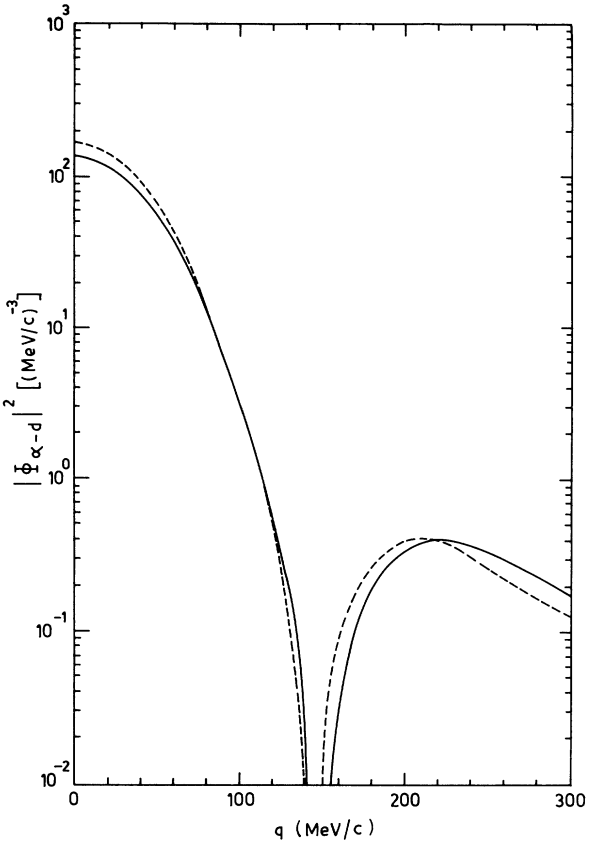

FIG. 8. The α-d internal momentum distribution of ^{6}Li. The solid curve is used for this analysis (see Ref. [4] for details). The dashed curve is obtained using Kukulin's wave function [18].

Since alphas are strongly absorbed particles, it is expected that the distortions of the incoming and outgoing wave functions caused by the presence of the residual nucleus will be important [1]. For (p,p') it was conjectured that the final-state interaction (FSI) might play an important role in explaining that data. Accordingly, we performed DWIA calculations which include most of the FSI except for the recombination effect in which the bound clusters recombine immediately after breakup.

For both the PWIA and DWIA analyses we have used the THREEDEE code of N. S. Chant. In both these theories the three-body knockout cross section for $A(a,a'b)B$ reaction takes a factorized form [14]

$$\frac{d^3\sigma}{d\Omega_a d\Omega_b dE_a} = \mathrm{KF}\{C^2S|\Phi(\mathbf{q})|^2\}\frac{d\sigma}{d\Omega}\Big|_{a-b} \quad (1)$$

where KF is a known kinematic factor, $(d\sigma/d\Omega)|_{a-b}$ is properly a half-off-the-energy-shell cross section for the interaction of particles a and b. The quantity C^2S represents the probability of finding the cluster b inside the target nucleus A and $\Phi(q)$ is the momentum distribution of the cluster b in the target A. In DWIA this $\Phi(q)$ is modified by distortion effects and is replaced by $\sum_\lambda T^{L\lambda}$, the so-called distorted momentum distribution given by

$$T^{L\lambda}=\frac{1}{(2L+1)^{1/2}}\int \chi_a^{(-)*}(\mathbf{r})\chi_b^{(-)*}(\mathbf{r})\Phi_{nLj}(\mathbf{r}) \times\chi_0^{(+)}\left[\frac{B}{A}\mathbf{r}\right]d\mathbf{r}\ , \tag{2}$$

where the χ's are the incoming and outgoing distorted waves and $\Phi_{nLj}(r)$ the bound cluster wave function in the ground state of the nucleus. In the plane-wave limit, $T^{L\lambda}$ is simply the Fourier transform of the cluster wave function.

In this analysis we have used the impulse approximation and therefore we have replaced the $(d\sigma/d\Omega)|_{a-b}$ by an appropriate on-shell two-body cross section. The final energy prescription (FEP) has been used because in previous studies [1,4] this prescription has been found to be most suitable.

In order to obtain the double-differential cross section corresponding to the inclusive measurement at a particular laboratory angle θ_1, we integrate over the solid angle of the unobserved particle

$$\frac{d^2\sigma}{d\Omega_a dE_a}=\int\frac{d^3\sigma}{d\Omega_a\, d\Omega_b\, dE_a}d\Omega_b\ . \tag{3}$$

For each θ_1 we find that there is a range of allowed θ_2, the scattering angle, and δ_2, the out-of-plane angle of the unobserved particle. Both q and $(d\sigma/d\Omega)|_{a-b}$ vary with δ_2 and θ_2. Therefore at each θ_1 we scan over a certain portion of the bound-state momentum wave function $\Phi(q)$.

The α-d bound-state wave function of ^{6}Li has been extensively investigated theoretically by many authors mostly using either a microscopic cluster model [15,16] or a three-body (αNN) model [17–19] based on the Faddeev formalism [20]. Both the cluster model and the three-body model predict an effective antisymmetrized S-wave function of the $2S$ form, i.e., a wave function that has a node. This $2S$ structure has been experimentally confirmed in the noncoplanar ^{6}Li(p,pd)^{4}He reaction by Warner *et al.* [21] and by ^{6}Li($e,e'd$)^{4}He reaction by Ent *et al.* [5]. In a knockout reaction it has been found that the shape of the momentum distribution at small momenta is determined by the tail of the bound-state wave function, and at larger recoil momenta the distortion effects tend to remove most of the large differences between different wave functions [4,10]. Since the alpha is a strongly absorbing particle, in an alpha-induced reaction a proper treatment of the asymptotic tail of the bound-state wave function by accurate inclusion of the Coulomb interaction is extremely important. Kukulin *et al.* recently solved the ^{6}Li three-body problem by the Faddeev formalism, including exact treatment of the Coulomb effect [18,19]. Warner *et al.*, in the analysis of (p,pd) data on ^{6}Li, took the bound-state wave function as the eigenfunction of a Woods-Saxon potential with the energy eigenvalue the same as the α-d separation energy [21,22] and found that the use of the properly antisymmetrized Kukulin wave function [18] produces identical results. In our analysis we have also used a Woods-Saxon wave function [4] and this wave function, as shown in Figs. 8 and 9, is virtually identical with that generated by

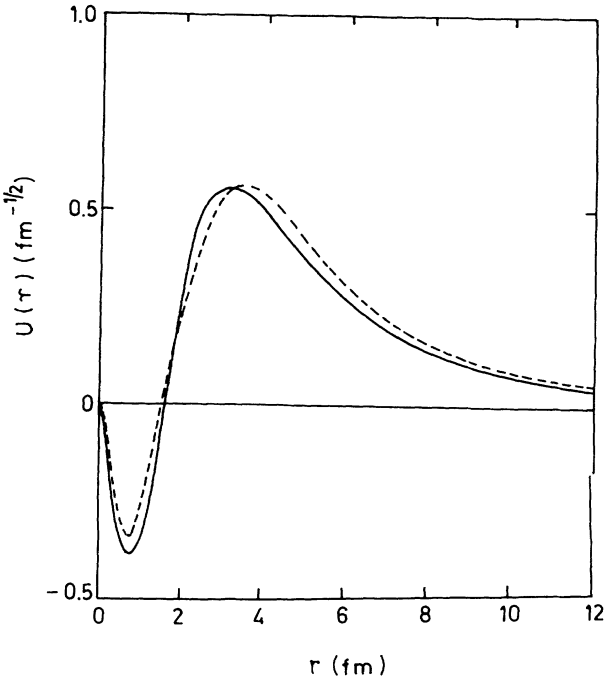

FIG. 9. The α-d bound-state wave function. The solid line corresponds to wave function generated in a Woods-Saxon potential and the dashed line to the Kukulin wave function [18].

Kukulin *et al.*

For the distorted-wave calculations the optical potential is of the form

$$V_{\rm opt}=-Vf(r,r_0,a) -i(W-4W_D a'd/dr')f(r,r',a')+V_{\rm Coul}$$

where

$$f(r,r_0,a)=\left[1-\exp\left[\frac{r-r_0A^{1/3}}{a}\right]\right]^{-1}$$

and $V_{\rm Coul}$ is the Coulomb potential of a uniform sphere of charge with radius $r_c A^{1/3}$, A being the target mass.

Starting with the parameters of Bragin *et al.* [23] obtained at $E_\alpha=50.5$ MeV we made a search of optical potential parameters. Figure 2 shows our ^{6}Li(α,α_0)^{6}Li (1^+, 0.0 MeV) elastic scattering data and the optical model calculations with the parameters given in Table I. The calculations fit our elastic data up to $\theta_{\rm c.m.}\sim 70°$. The rise in the cross section beyond this angle is well understood in terms of the exchange effect [23] which is not incorporated in our optical model calculations. In Fig. 5 we show the angular distribution of the 3^+, 2.185 MeV excited state of ^{6}Li along with the DWBA calculations using the same optical potential parameters as given in Table I. The calculations were carried out using the code DWUCK4 [24]. We have used the deformation parameter $\beta=0.45$ to normalize our DWBA calculations with the data. This is in reasonable agreement with those obtained from the theoretical $B(E2)$ values given in Ref. [25]. Although the fit is not very good, it reproduces the overall structure

TABLE I. Optical-potential parameters.

Reaction	E	System	V^a	r_0	a	r_c	W	W_D	r_0'	a'	Ref.
^{6}Li($\alpha,2\alpha$)^{2}H	50.0	$\alpha+^6$Li	85.98	1.15	0.8	1.3	0.0	14.01	1.7	0.657	b
	52.0	$d+\alpha$	103.16 $-0.5E$	1.05	0.775	1.3	0.0	8.174	1.28	0.741	[26]
	Bound state		77.0	1.47	0.71	1.47	0.0				[4]
^{6}Li($\alpha,\alpha d$)α	50.0	$\alpha+^6$Li	85.98	1.15	0.8	1.3	0.0	14.01	1.7	0.657	b
	47.1	$\alpha+\alpha$	107.0	1.14	0.7	1.14	1.0	0.0	1.14	0.7	[27]

[a]In the distorted-wave impulse approximation calculation for the reaction $A(a,a'b)B$, the well depth V for $\alpha+^6$Li was multiplied by B/A to crudely exclude the interaction between the incoming α and the knocked-out particle.
[b]This work.

of the angular distribution. The possible effect of alpha-cluster exchange leading to the excited state of ^{6}Li has not been investigated here. Appropriate consideration of this effect might produce a better fit to the data.

In our DWIA calculations, the optical-potential parameters used for the $\alpha+^6$Li entrance channel are given in Table I. In the outgoing channel for the ^{6}Li($\alpha,2\alpha$)^{2}H reaction we have one alpha with very high energy (due to our selection of the energy bin near the α-d threshold) close to the elastic α energy and the other with relatively low energy. For the high-energy scattered α in the α-d channel we have used the energy-dependent optical-potential parameters of Hinterberger *et al.* [26]. For the ^{6}Li($\alpha,\alpha d$)^{4}He reaction in the $\alpha+^4$He channel, we have used the optical-potential parameters obtained at $E_\alpha=47.10$ MeV [27].

Since in an inclusive measurement only one of the particles is detected, the wave function of the unobserved particle cannot be complex and should be calculated in a purely real potential [28]. It should be noted that since the kinematics and the phase-space factor require the unobserved particle to make a transition to the continuum, Pauli blocking is automatically included. Because we have confined our measurements to the high energy scattered α-particle region, the energy of the unobserved particle is extremely low where optical-potential parameters are not available. Therefore we have retained only the Coulomb potential between the unobserved particle and the residual nucleus, assuming very little nuclear interference at this low energy.

To estimate the QF contribution in our (α,α') data, we have considered both the ^{6}Li($\alpha,2\alpha$)^{2}H and ^{6}Li($\alpha,\alpha d$)^{4}He reactions at $E_\alpha=50$ MeV. In these reactions, α-α two-body and α-d two-body interactions are expected to play dominant roles. In our inclusive cross-section calculation we find that at each θ_1, the unobserved particle can have a wide range of θ_2 and δ_2 and the corresponding effective two-body laboratory energy may differ considerably from 50 MeV. The α-α and α-d two-body cross sections have been taken at appropriate effective laboratory energies and c.m. angles (from the FEP) using a smooth interpolation of the available α-α data in the energy range 29–53 MeV [29–31] and the α-d data in the range 30–52 MeV [26,32]. In these energy regions both α-α and α-d two-body cross sections vary rapidly with energy and angle. From Eqs. (1) and (3) we find that we have to integrate over various values of $(d\sigma/d\Omega)|_{a-b}$ and therefore a comparison of the contribution of the ^{6}Li($\alpha,2\alpha$) and ^{6}Li($\alpha,\alpha d$) reactions cannot be made just on the basis of the relative magnitudes of α-α and α-d two-body cross sections at $E_\alpha=50$ MeV. However, with the increase of θ_1, the $q=0$ point (at which the maximum of the cross section occurs) corresponding to the $(\alpha,\alpha d)$ reaction moves more rapidly towards lower scattered alpha energies than for the $(\alpha,2\alpha)$ reaction. Therefore, as θ_1 increases, we find less and less $(\alpha,\alpha d)$ reaction contribution to our data.

The PWIA and DWIA calculations for the ^{6}Li($\alpha,2\alpha$) reaction (with different normalizations) are shown in Fig. 6. The normalization factor for the PWIA calculation is 0.14. This is consistent with the values of 0.08–0.20 found from analysis of ^{6}Li($\alpha,2\alpha$) reactions using various wave functions [1–3]. In Fig. 6 the solid curve represents the DWIA calculations with a normalizing constant (spectroscopic factor) of 1.0 which is close to the microscopic estimate of 0.93 [33]. The spectroscopic factor obtained from the ^{6}Li($e,e'd$)^{4}He reaction, where distortion effects are expected to be minimum, is 0.73 ± 0.09 [5]. The best overall fit to our data seems to correspond to a higher normalization constant. DWIA calculations with a normalization constant of 1.8 seem to be in reasonable agreement with the data as shown by the dash-dotted curve in Fig. 6. The uncertainty in the spectroscopic factor arises mainly from the uncertainty of the optical-potential parameters especially because they are not well determined for a few nucleon systems. Moreover, it has already been observed that in the alpha-particle-induced cluster knock-out reactions the DWIA calculations reproduce the shape of the angular and energy-sharing distributions but they usually overpredict the spectroscopic factors [10,34]. We find that both the PWIA and DWIA calculations for the ^{6}Li($\alpha,2\alpha$) reaction agree well with the general trend of the data for $\theta_{\rm lab}\simeq11°$ to 30°. The DWIA calculations give a deeper first minima in the angular distribution and the peak near $\theta_{\rm lab}\sim25°$ is slightly shifted from the one obtained in PWIA calculations. At angles $\theta_{\rm lab}<11°$ the experimentally obtained cross sections are much less than the calculated values. This decrease in cross sections at forward angles is not due to the effect of distortions because both

PWIA and DWIA show a sharp rise in cross section in this region and a variation in normalization does not account for this discrepancy. At $\theta_{lab} > 30°$ the calculated cross sections underpredict the measured values. By adding the contributions from the ^{6}Li$(\alpha,\alpha d)^4$He reaction incoherently with the ^{6}Li$(\alpha,2\alpha)^2$H results, we find that this increases the total calculated cross section by $\sim 20\%$ at $\theta_{lab} = 12.5°$, $\sim 10\%$ at 22.5°, $\sim 4\%$ at 30°, and even less at larger angles. This clearly, therefore, cannot resolve the observed discrepancy, i.e., overpredicting the cross sections below $\theta_{lab} \sim 11°$ and underpredicting the cross section above 30°.

The most striking feature that comes out of this analysis is the failure of the quasifree reaction mechanism near $q \sim 0$. This feature was also observed in the ^{6}Li(p,p') reaction where similar overpredictions of quasifree scattering calculations were found for $\theta_{lab} \leq 25°$ (i.e., $\theta_{c.m.} \leq 30°$) [9]. We find that for our (α,α') data at $E_\alpha = 50$ MeV, the momentum transferred to the system by the projectile is ~ 117 MeV/c at $\theta_{lab} = 11°$. The same value of momentum transfer is obtained for the (p,p') data at $E_p = 65$ MeV, when $\theta_{lab} \sim 19.5°$ the angle where the experimental cross section reaches its maximum. It seems therefore that the onset of discrepancy in both ^{6}Li(p,p') and ^{6}Li(α,α') reactions corresponds to roughly the same magnitude of momentum transfer.

It should be noted that by our choice of data window at the high energy part of the continuum we are observing the low energy transfer, i.e., the relative energy of the broken up α-d pair is small. The above observation possibly indicates that at forward angles either the QF mechanism does not work for small relative energy or some other reaction mechanism (such as strong final state interactions leading to recombination of the α-d clusters) contributes to lowering the cross section. It would also be interesting to see the effect of the proper treatment of the coupling term in the DWIA calculations [35].

B. DWBA analysis

Although the DWIA takes care of most of the final-state interactions (FSI) between the outgoing particles and the residual nucleus, it does not include recombination effects. Of course, if the recombination between the knocked-out particle and the residual nucleus occurs on a long time scale, the scattered α particle remains unaffected and this would have no effect on the inclusive spectra. On the other hand, if the recombination occurs on a very short time scale producing a two-body final state instead of a three-body system, this would affect the kinematics of the scattered α particle. Because of the special choice of kinematics selected for our data reduction, there is very little energy left for the bound α and d clusters. Due to this constraint, the α and d will not separate after breakup. In fact we may visualize this as if the interaction between the projectile and the target excites the target to a virtual state (1.475 MeV, in our case), and the bound clusters do not get separated after the scattering, thereby producing a two-body final state.

With this in mind we have carried out a distorted-wave Born approximation (DWBA) analysis of our data. The ground state of ^{6}Li has $J^\pi = 1^+$ with α-d relative angular momentum predominantly $L = 0$ [5]. The spin and parity of this virtual excited state are also assumed to be 1^+, which is a possible configuration if the relative angular momentum L between the clusters is 2 instead of 0. The DWBA analysis of this 1^+, 1.47 MeV state has been done using the parameter set 1 of Table I, with the code DWUCK4 [24]. To normalize the calculations with the data we have used an arbitrary normalization factor which corresponds to $\beta = 0.19$. In Fig. 7 we find that though the DWBA calculations are unable to explain the full angular distribution, they do produce a reduction of the cross section at forward angles.

IV. DISCUSSIONS

We studied the ^{6}Li(α,α') reaction at $E_\alpha = 50$ MeV to examine the mechanism of ^{6}Li breakup into $\alpha + d$ clusters at small relative energy. We selected a region of excitation energy 1 MeV wide starting at the α-d breakup threshold, and measured its angular distribution. We find that the data show a sharp rise in cross section with decreasing scattering angle up to about $\theta_{lab} \sim 11°$ ($\theta_{c.m.} \sim 20°$). We analyzed the data in the framework of the quasifree reaction mechanism and performed impulse approximation calculations. The DWIA shows fair agreement with the general trend of the observed cross sections between laboratory angles of 11° and 30°. At forward angles ($\theta_{lab} \leq 11°$) both the PWIA and DWIA calculations show a continuous rise in cross section in contrast to the data. At scattering angles greater than $\theta_{lab} = 30°$, the PWIA and DWIA calculations both underpredict the observed cross section. These larger angles correspond to the larger relative momenta (q) for the bound α-d clusters, and the failure of impulse-approximation calculations for cluster knockout reactions at large q has been observed before [1,10,34]. The important finding of our work is that standard impulse-approximation calculations fail to reproduce the observed data at forward angles (near $q \sim 0$) where the quasifree mechanism is expected to be most valid. Similar phenomena were also observed in the ^{6}Li(p,p') reaction [9] in which the experimental cross sections showed a significant deviation from the plane-wave impulse-approximation calculations for $\theta_{lab} \leq 25°$ (i.e., $\theta_{c.m.} \leq 30°$). For the ^{6}Li(p,p') data, the experimental cross sections were found to reach their maximum values at $\theta_{lab} \sim 20°$. Whereas, in the ^{6}Li(α,α') data this maximum occurs at $\theta_{lab} \sim 11°$. It is pertinent to note that both angles correspond to nearly the same magnitude of momentum transfer for the two reactions. This possibly indicates the breakdown of the quasifree breakup reaction mechanism for small relative energies for the outgoing particles when the momentum transfer falls below a critical value. Since the alpha is a strongly absorbed particle, we have carried out distorted-wave-impulse-approximation (DWIA) calculations. But we find that the reduction in cross sections at the forward angles is not an effect caused by the distortions. The DWIA used in our analysis include most of the final-state interactions (FSI) except for recombination. Possibly a full Faddeev three-body calculation for

the continuum, including the FSI, is needed.

As a first attempt to understand the effects of this recombination we performed DWBA calculations assuming excitation of a virtual state at the breakup threshold. The DWBA calculations do show a sharp decrease in cross section for $\theta_{\text{lab}} \leq 11°$ but comparison with the overall angular distribution data reflects the inadequacies of the DWBA calculations. Recombination effects could possibly be studied by coupling the 1^+(g.s.)-3^+-continuum (C^+) states with all possible reorientation terms in a conventional coupled-channel calculation. These calculations, along with the alpha-cluster exchange phenomena, properly incorporated, might provide a better understanding of both our elastic and inelastic data. Additionally, experimental data on the ^{6}Li(d,d') reaction near the α-d breakup threshold would be useful. A comparison of the (d,d') data with the (α,α') and (p,p') work may provide further insight into the breakdown of the QF formalism and a possible change in the reaction mechanism below a critical value of momentum transfer.

ACKNOWLEDGMENTS

It is a pleasure to thank the detector and the target laboratory personnel as well as the operating staff of the Cyclotron and the Computer of the Variable Energy Cyclotron Center for their kind assistance. We would also like to thank Dr. B. C. Sinha, VECC, Calcutta and Professor H. Rebel, KFK, Karlsruhe for their generous help in the experiment. One of us (C.S.) is thankful to Dr. H. P. Blok, Vrije Universiteit, Amsterdam, for helpful discussions.

[1] J. W. Watson, H. G. Pugh, P. G. Roos, D. A. Goldberg, R. A. J. Riddle, and D. I. Bonbright, Nucl. Phys. **A172**, 513 (1971); M. Jain, P. G. Roos, H. G. Pugh, and H. D. Holmgren, *ibid.* **A153**, 49 (1970); J. R. Pizzi, M. Gaillard, P. Gaillard, A. Guichard, M. Gusakow, G. Reboulet, and C. Ruhla, *ibid.* **A136**, 496 (1969).

[2] J. M. Lambert, R. J. Kane, P. A. Treado, L. A. Beach, E. L. Petersen, and R. B. Theus, Phys. Rev. C **4**, 2010 (1971).

[3] A. K. Jain, J. Y. Grossiord, M. Chevallier, P. Gaillard, A. Guichard, M. Gusakow, and J. R. Pizzi, Nucl. Phys. **A216**, 519 (1973); R. Hagelberg, E. L. Haase, and Y. Sakamoto, *ibid.* **A207**, 366 (1973).

[4] P. G. Roos, D. A. Goldberg, N. S. Chant, R. Woody III, and W. Reichart, Nucl. Phys. **A257**, 317 (1976); P. G. Roos, N. S. Chant, A. A. Cowley, D. A. Goldberg, H. D. Holmgren, and R. Woody III, Phys. Rev. C **15**, 69 (1977).

[5] R. Ent, H. P. Blok, J. F. A. Van Hienen, G. Van der Steenhoven, J. F. J. Van den Brand, J. W. A. den Herder, E. Jans, P. H. M. Keizer, L. Lapikas, E. N. M. Quint, P. K. A. de Witt Huberts, B. L. Berman, W. J. Briscoe, C. T. Christou, D. R. Lehman, B. E. Norum, and A. Saha, Phys. Rev. Lett. **57**, 2367 (1986).

[6] J. R. Hurd, J. S. Boswell, R. C. Minehart, Y. Tzeng, H. J. Ziock, K. O. Ziock, L. C. Liu, and E. R. Siciliano, Nucl. Phys. **A475**, 743 (1987).

[7] H. Jelitto, J. Buschmann, V. Corcalciuc, H. J. Gils, N. Heide, J. Kiener, H. Rebel, C. Samanta, and S. Zagromski, Z. Phys. A **332**, 317 (1989).

[8] N. Heide, H. Rebel, V. Corcalciuc, H. J. Gils, H. Jelitto, J. Kiener, J. Wentz, S. Zagromski, and D. K. Srivastava, Nucl. Phys. **A504**, 374 (1989).

[9] M. Tosaki, M. Fujiwara, K. Hosono, T. Noro. H. Ito, T. Yamazaki, and H. Ikegami, Nucl. Phys. **A493**, 1 (1989).

[10] C. Samanta, N. S. Chant, P. G. Roos, A. Nadasen, and A. A. Cowley, Phys. Rev. C **26**, 1379 (1982); C. Samanta, N. S. Chant, P. G. Roos, A. Nadasen, J. Wesick, and A. A. Cowley, *ibid.* **34**, 1610 (1986); C. Samanta, N. S. Chant, P. G. Roos, A. Nadasen, and A. A. Cowley, *ibid.* **35**, 333 (1987).

[11] A. Nadasen, T. A. Carey, P. G. Roos, N. S. Chant, C. W. Wang, and H. L. Chen, Phys. Rev. C **19**, 2099 (1979).

[12] F. Ajzenberg-Selove, Nucl. Phys. **A490**, 1 (1990) (see Table 6.2, page 33).

[13] J. C. Bergstrom and E. L. Tomusiak, Nucl. Phys. **A262**, 196 (1976).

[14] N. S. Chant and P. G. Roos, Phys. Rev. C **15**, 57 (1977).

[15] I. V. Kurdyumov, V. C. Neudatchin, and Yu. F. Smirnov, Phys. Lett. **31B**, 426 (1970); Yu. A. Kudeyarov, I. V. Kurdyumov, V. G. Neudatchin, and Yu. F. Smirnov, Nucl. Phys. **A163**, 316 (1971).

[16] R. G. Lovas, A. T. Kruppa, R. Beck, and F. Dickmann, Nucl. Phys. **A474**, 451 (1987).

[17] D. R. Lehman and M. Rajan, Phys. Rev. C **25**, 2743 (1982); W. C. Parke and D. R. Lehman, *ibid.* **29**, 2319 (1984); C. T. Christou, C. J. Seftor, W. J. Briscoe, W. C. Parke, and D. R. Lehman, *ibid.* C **31**, 250 (1985).

[18] V. I. Kukulin, V. M. Krasnopol'sky, V. T. Voronchev, and P. B. Sazonov, Nucl. Phys. **A417**, 128 (1984).

[19] V. I. Kukulin, V. T. Voronchev, T. D. Kaipov, and R. A. Eramzhyan, Nucl. Phys. **A517**, 221 (1990).

[20] L. D. Faddeev, Zh. Eksp. Teor. Fiz. **39**, 1459 (1960) [Sov. Phys. JETP **12**, 1014 (1961)].

[21] R. E. Warner, R. S. Wakeland, J-Q. Yang, D. L. Friesel, P. Schwandt, G. Caskey, A. Galonsky, B. Remington, and A. Nadasen, Nucl. Phys. **A422**, 205 (1984).

[22] R. E. Warner, J-Q. Yang, D. L. Friesel, P. Schwandt, G. Caskey, A. Galonsky, B. Remington, A. Nadasen, N. S. Chant, F. Khazaie, and C. Wang, Nucl. Phys. **A443**, 64 (1985).

[23] V. N. Bragin, N. T. Burtebaev, A. D. Duisebaev, G. N. Ivanov, S. B. Sakuta, V. I. Chuev, and L. V. Chuakov, Yad. Fiz. **44**, 312 (1986) [Sov. J. Nucl. Phys. **44**, 198 (1986)].

[24] P. D. Kunz, computer code DWUCK4 (unpublished).

[25] F. Petrovich, R. H. Howell, C. H. Poppe, S. M. Austin, and G. M. Crawley, Nucl. Phys. **A383**, 355 (1982) (see references therein).

[26] P. Hinterberger, G. Mairle, U. Schmidt-Roor, G. J. Wagner, and P. Turek, Nucl. Phys. **A111**, 265 (1968).

[27] G. Igo, Phys. Rev. **117**, 1079 (1960).

[28] J. S. Wesick, P. G. Roos, N. S. Chant, C. C. Chang, A. Nadasen, L. Rees, N. R. Yoder, A. A. Cowley, S. J. Mills,

and W. W. Jacobs, Phys. Rev. C **32**, 1474 (1985).
[29] H. E. Conzett, G. Igo, H. C. Shaw, and R. J. Slobodrian, Phys. Rev. **117**, 1075 (1960).
[30] P. Darriulat, G. Igo, H. G. Pugh, and H. D. Holmgren, Phys. Rev. **137**, B315 (1965).
[31] D. J. Bredin, W. E. Burcham, D. Evans, W. M. Gibson, J. S. C. McKee, D. J. Prowse, J. Rotblat, and J. N. Snyder, Proc. R. Soc. London **A251**, 143 (1959).
[32] H. Willmes, C. R. Messick, T. A. Cahill, D. J. Shadoan, and R. G. Hammond, Phys. Rev. C **10**, 1762 (1974).
[33] K. Varga and R. G. Lovas, Phys. Rev. C **43**, 1201 (1991).
[34] C. W. Wang, N. S. Chant, P. G. Roos, A. Nadasen, and T. A. Carey, Phys. Rev. C **21**, 1705 (1980).
[35] A. K. Jain, Phys. Rev. C **42**, 368 (1990).